

A Multi-Class Lane-Changing Advisory System for Freeway Merging Sections Using Cooperative ITS

Sharma, Salil; Papamichail, Ioannis; Nadi, Ali; van Lint, Hans; Tavasszy, Lorant; Snelder, Maaïke

DOI

[10.1109/TITS.2021.3137233](https://doi.org/10.1109/TITS.2021.3137233)

Publication date

2021

Document Version

Final published version

Published in

IEEE Transactions on Intelligent Transportation Systems

Citation (APA)

Sharma, S., Papamichail, I., Nadi, A., van Lint, H., Tavasszy, L., & Snelder, M. (2021). A Multi-Class Lane-Changing Advisory System for Freeway Merging Sections Using Cooperative ITS. *IEEE Transactions on Intelligent Transportation Systems*, 23(9), 15121-15132. <https://doi.org/10.1109/TITS.2021.3137233>

Important note

To cite this publication, please use the final published version (if applicable).
Please check the document version above.

Copyright

Other than for strictly personal use, it is not permitted to download, forward or distribute the text or part of it, without the consent of the author(s) and/or copyright holder(s), unless the work is under an open content license such as Creative Commons.

Takedown policy

Please contact us and provide details if you believe this document breaches copyrights.
We will remove access to the work immediately and investigate your claim.

Green Open Access added to TU Delft Institutional Repository

'You share, we take care!' - Taverne project

<https://www.openaccess.nl/en/you-share-we-take-care>

Otherwise as indicated in the copyright section: the publisher is the copyright holder of this work and the author uses the Dutch legislation to make this work public.

A Multi-Class Lane-Changing Advisory System for Freeway Merging Sections Using Cooperative ITS

Salil Sharma¹, Ioannis Papamichail², Ali Nadi, Hans van Lint,
Lóránt Tavasszy³, *Member, IEEE*, and Maaïke Snelder

Abstract—Cooperative intelligent transportation systems (C-ITS) support the exchange of information between vehicles and infrastructure (V2I or I2V). This paper presents an in-vehicle C-ITS application to improve traffic efficiency around a merging section. The application balances the distribution of traffic over the available lanes of a freeway, by issuing targeted lane-changing advice to a selection of vehicles. We add to existing research by embedding multiple vehicle classes in the lane-changing advisory framework. We use a multi-class multi-lane macroscopic traffic flow model to design a feedback-feedforward control law that is based on a linear quadratic regulator (LQR). The weights of the LQR controller are fine-tuned using a response surface method. The performance of the proposed system is evaluated using a microscopic traffic simulator. The results indicate that the multi-class lane-changing advisory system is able to suppress shockwaves in traffic flow and can significantly alleviate congestion. Besides bringing substantial travel time benefits around merging sections of up to nearly 21%, the system dramatically reduces the variance of travel time losses in the system. The proposed system also seems to improve travel times for mainline and ramp vehicles by nearly 20% and 42%, respectively.

Index Terms—Lane-changing advisory, LQR control method, merging section, multi-class, traffic flow modeling, cooperative intelligent transportation system.

I. INTRODUCTION

TRAFFIC congestion on freeways causes large delays and therewith high societal costs. Infrastructural bottlenecks (e.g., merging sections, lane-drops, work zones, etc.) locally

Manuscript received January 26, 2021; revised July 22, 2021; accepted November 24, 2021. This work was supported in part by the Netherlands Organization for Scientific Research (NWO), in part by the Dutch Institute for Advanced Logistics (TKI Dinalog), in part by the Commit2data, in part by the Port of Rotterdam, in part by the SmartPort, in part by the Portbase, in part by Transport en Logistiek Nederland (TLN), in part by the Deltalinqs, in part by the Rijkswaterstaat, and in part by Nederlandse Organisatie voor Toegepast Natuurwetenschappelijk Onderzoek (TNO) under Project ToGRIP-Grip on Freight Trips. The Associate Editor for this article was C. G. Claudel. (*Corresponding author: Salil Sharma.*)

Salil Sharma, Ali Nadi, Hans van Lint, and Lóránt Tavasszy are with the Department of Transport and Planning, Faculty of Civil Engineering and Geosciences, Delft University of Technology, 2628 Delft, The Netherlands (e-mail: s.sharma-4@tudelft.nl; a.nadinajafabadi@tudelft.nl; j.w.c.vanlint@tudelft.nl; l.a.tavasszy@tudelft.nl).

Ioannis Papamichail is with the Dynamic Systems and Simulation Laboratory, School of Production Engineering and Management, Technical University of Crete, 73100 Chania, Greece (e-mail: ipapa@dssl.tuc.gr).

Maaïke Snelder is with the Department of Transport and Planning, Faculty of Civil Engineering and Geosciences, Delft University of Technology, 2628 Delft, The Netherlands, and also with TNO, 2595 The Hague, The Netherlands (e-mail: m.snelder@tudelft.nl).

Digital Object Identifier 10.1109/TITS.2021.3137233

cause congestion that may spill back to other parts of the network. When traffic demand exceeds the capacity of a merging section, it becomes an active bottleneck which results in the formation of a queue on the near-side lane of a mainline carriageway. The queue then spreads laterally to other lanes and triggers a drop in the discharge flow or a phenomenon known as capacity drop [1], [2]. Data from several studies suggest that traffic flow is unevenly distributed over available lanes of a freeway [3]–[5]. Around a merging section, unbalanced flow distribution might also contribute to traffic breakdown on a heavily used lane (i.e. near-side lane) while there is spare capacity available on the other lanes.

In recent years, technological breakthroughs in communication and automation have enabled us to research and develop new cooperative intelligent transportation system (C-ITS) solutions to help tackle the problem of congestion. This system enables vehicles to exchange relevant information with other vehicles (V2V) or with the road infrastructure (V2I or I2V) using communication technology in order to create in-vehicle and cooperative systems [6]. Using C-ITS, this paper presents an in-vehicle lane-changing advisory system that aims at improving traffic efficiency by balancing the distribution of traffic flow around merging sections.

Existing research has recognized that the traffic situation in the vicinity of infrastructural bottlenecks can be improved by efficiently assigning traffic flow to available lanes on freeways. Rule-based approaches are proposed in [7] and [8] where vehicles are advised a suitable lane in the vicinity of bottlenecks. Although these approaches can be applied in real-time, they require enough knowledge about the traffic system to generate a set of instructions. In [9]–[11], the lane assignment problem is treated as an optimization program. However, the inherent computational processing time associated with these approaches might hinder their real-time applicability. In contrast to the above approaches, several approaches based on the optimal control theory have been proposed in [12]–[16]. These approaches can be implemented in real-time and do not require a set of rules for operations, thus alleviating the limitations of rule-based and optimization-based approaches. However, previous studies solely focus on passenger cars and do not embed multiple vehicle classes in the lane-changing advisory framework. Heterogeneity induced from class-specific properties can affect traffic efficiency [17]. This paper addresses this research gap by incorporating multiple vehicle classes by means of passenger car equivalents within a

multi-class multi-lane macroscopic traffic flow model. We use this traffic flow model to design a multi-class lane-changing advisory system based on a linear quadratic regulator (LQR).

Controllers can be designed in a way to guarantee stability in the sense that they often have tunable parameters that affect how the controlled system stabilizes. In this respect, an LQR controller contains two weighting matrices that regulate the penalties with respect to state variables and control actions. These weights are selected by a designer and affect the behavior of the LQR controller. In [12]–[16], these weights are selected using trial-and-error-based approaches. Other classical approaches include Bryson’s method [18] and pole placement [19]. However, these approaches are often time-consuming and labor-intensive processes. Some studies have formulated the selection of weighting matrices for an LQR controller as an optimization problem and solved it using meta-heuristics [20]–[23]. These methods can explore the search space in an informed manner and converge to the optimal solutions. Compared to optimization-based approaches, the response surface method can reveal meaningful information from a small number of experiments. Approximation or meta-models can be developed to map the relationship between performance characteristics and design variables in order to determine the optimum design parameters [24], [25]. In this paper, we adopt the response surface method to find these weighting matrices that ensure a robust performance for an LQR controller.

Further, we use microscopic simulation to evaluate the performance of the proposed controller around merging sections, in contrast to [15] and [16], since a microscopic traffic simulator provides a real-world testbed to test an in-vehicle lane-changing advisory system.

To this end, the objective of this study is to propose a multi-class lane-changing controller around a merging section to improve its traffic efficiency. To the best of our knowledge, this is the first multi-class LQR controller for lane-changing. This paper contributes to the existing literature by:

- 1) developing a multi-class lane-changing advisory system based on a linear quadratic regulator (LQR);
- 2) performing a response surface-based approach to select the optimal weights of the LQR controller; and
- 3) evaluating the performance of the LQR controller around a merging section using a microscopic traffic simulator.

This paper is structured as follows. We formulate a multi-class lane-changing LQR controller in Section II. Next, Section III describes the approach to implement the proposed controller in microscopic simulation software. Then, Section IV describes the experimental setup to evaluate the proposed controller. In section V, we describe the optimum selection of set points and the weights of the LQR controller. We present and discuss our results in Section VI. Finally, we conclude the paper and discuss future works in Section VII.

II. FORMULATING A MULTI-CLASS LANE-CHANGING LQR CONTROLLER

This section first develops a linear time invariant system based on a multi-class multi-lane traffic flow model. Then,

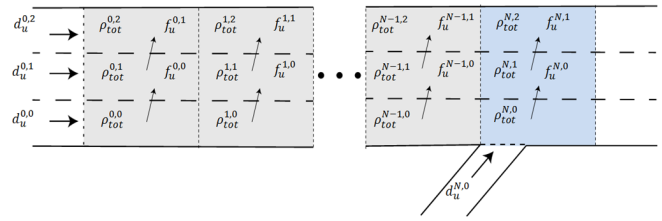


Fig. 1. A hypothetical freeway stretch with an on-ramp.

we formulate an LQR controller. Lastly, we discuss the possible implementation of this LQR controller as a C-ITS based application.

A. Traffic System Dynamics Using a Multi-Class Multi-Lane Traffic Flow Model

Based on a linear multi-lane traffic flow model proposed in [13], we consider a multilane freeway as shown in Fig. 1. The freeway is divided into $i = 0, \dots, N$ segments of length L_i . Each such segment is composed of $j = m_i, \dots, M_i$ lanes, where m_i and M_i denote the minimum and maximum indices of lanes for segment i . It is assumed that $j = 0$ corresponds to the segment(s) on the rightmost lane. In Fig. 1, $m_0 = 0$ and $M_0 = 2$. Each element of the resulting grid is termed as a cell with index (i, j) . According to the definition, the total number of cells from the origin to segment i is $H_i = \sum_{r=0}^i (M_r - m_r + 1)$, and the total number of cells for the whole stretch is $\overline{H} = H_N$. To formulate the model in discrete time, we consider the discrete-time step T , indexed by $k = 0, 1, \dots$, where the time is $t = kT$.

First of all, we will focus on defining the dynamics of a multi-class traffic system comprising U number of vehicle classes. For every vehicle class u , the conservation of vehicles can be defined as:

$$\frac{\partial \rho_u}{\partial t} + \frac{\partial q_u}{\partial x} = 0, \quad (1)$$

where ρ_u and q_u refer to the class-specific density and class-specific flow at time t and location x , respectively.

Under assumptions of homogeneous and stationary conditions, class-specific density and flow are related, according to the continuity equation, as

$$q_u = \rho_u v_u, \quad (2)$$

where v_u refers to the class-specific average speed and can be expressed as $v_u = V_u^e(\rho_{tot})$. Here, V_u^e denotes the class-specific equilibrium speed which is a function of the total effective density ρ_{tot} in pce/km. ρ_{tot} is described by a function of the class-specific densities (ρ_u) and the dynamic pce values (η_u) and reads $\rho_{tot} = \sum_u \eta_u \rho_u$. This dynamics shows in a simple way that controlling (effective) densities of user class u naturally affects the speed and in turn the (effective) densities of all other classes [17].

Now, the evolution of density for every vehicle class u in a cell (i, j) , proposed in (1), can be cast in discrete form as

$$\begin{aligned} \rho_u^{i,j}(k+1) &= \rho_u^{i,j}(k) + \frac{T}{L_i} \left(q_u^{i-1,j}(k) - q_u^{i,j}(k) \right) \\ &\quad + \frac{T}{L_i} \left(f_u^{i,j-1}(k) - f_u^{i,j}(k) \right) + \frac{T}{L_i} d_u^{i,j}(k), \quad (3) \end{aligned}$$

where $\rho_u^{i,j}(k)$ is the density of vehicle class u in a cell (i, j) at time instant k ; $q_u^{i,j}(k)$ is the longitudinal flow of vehicle class u leaving cell (i, j) and entering cell $(i+1, j)$ during the time interval $[k, k+1)$; $f_u^{i,j}(k)$ is the net lateral flow of vehicle class u leaving cell (i, j) and entering cell $(i, j+1)$ during time interval $[k, k+1)$; and $d_u^{i,j}(k)$ is the external flow of vehicle class u entering the network in cell (i, j) either from mainline or an on-ramp during the time interval $[k, k+1)$.

The discretization should also satisfy the following Courant–Friedrichs–Lewy CFL condition:

$$\frac{L_i}{T} \geq \max \left\{ v_u^{i,j} \right\}_{u=1, \dots, U} \quad (4)$$

Since each cell has a mix of vehicle classes, the effective density of a cell (i, j) can be defined using passenger car-equivalents (pce) of vehicle classes:

$$\rho_{tot}^{i,j}(k) = \sum_u \eta_u^{i,j}(k) \rho_u^{i,j}(k), \quad (5)$$

where $\rho_{tot}^{i,j}(k)$ is the effective density of a cell (i, j) at time instant k [pce/km]; and $\eta_u^{i,j}(k)$ is the passenger car equivalent for a vehicle class u in a cell (i, j) at time instant k .

Similarly, total flow in passenger car-equivalents in a cell (i, j) can be defined as:

$$q_{tot}^{i,j}(k) = \sum_u \eta_u^{i,j}(k) q_u^{i,j}(k), \quad (6)$$

where $q_{tot}^{i,j}(k)$ is the total longitudinal flow of vehicle class u leaving cell (i, j) and entering cell $(i+1, j)$ during time interval $[k, k+1)$ [pce/h]; and $\eta_u^{i,j}(k)$ is the passenger car equivalent for a vehicle class u in a cell (i, j) at time instant k .

By combining (3), (5), and (6), the evolution of the effective density of a cell (i, j) can be expressed as

$$\begin{aligned} \rho_{tot}^{i,j}(k+1) = & \sum_u \left\{ \eta_u^{i,j}(k) \rho_u^{i,j}(k) \right. \\ & + \frac{T}{L_i} \left(\eta_u^{i-1,j}(k) q_u^{i-1,j}(k) - \eta_u^{i,j}(k) q_u^{i,j}(k) \right) \\ & + \frac{T}{L_i} \left(\eta_u^{i,j-1}(k) f_u^{i,j-1}(k) - \eta_u^{i,j}(k) f_u^{i,j}(k) \right) \\ & \left. + \frac{T}{L_i} \eta_u^{i,j}(k) d_u^{i,j}(k) \right\}. \quad (7) \end{aligned}$$

Depending on the network topology, some terms in the above equation may not be present. Lateral flows $f_u^{i,j}$ only exist for $m_i \leq j < M_i$. Thus, the total number of lateral flows are computed as $\overline{F} = U(\overline{H} - N)$.

Recall the relationship between macroscopic traffic flow parameters:

$$q_u^{i,j}(k) = \rho_u^{i,j}(k) \cdot v_u^{i,j}(k). \quad (8)$$

Combining (7) and (8), we get

$$\begin{aligned} \rho_{tot}^{i,j}(k+1) = & \sum_u \left\{ \left(1 - \frac{T}{L_i} v_u^{i,j}(k) \right) \eta_u^{i,j}(k) \rho_u^{i,j}(k) \right. \\ & + \frac{T}{L_i} \left(\eta_u^{i-1,j}(k) v_u^{i-1,j}(k) \rho_u^{i-1,j}(k) \right) \\ & + \frac{T}{L_i} \left(\eta_u^{i,j-1}(k) f_u^{i,j-1}(k) - \eta_u^{i,j}(k) f_u^{i,j}(k) \right) \\ & \left. + \frac{T}{L_i} \eta_u^{i,j}(k) d_u^{i,j}(k) \right\}. \quad (9) \end{aligned}$$

The proposed control actions are intended for usage before the possible onset of congestion, aiming to delay or avoid it. In this case, we may assume that the overall traffic flow entering the controlled area is bounded as it does not exceed the bottleneck capacity (e.g., using a variable speed limit controller for mainline traffic) and the proposed controller itself can avoid the creation of congestion. We can put forward the following assumptions to simplify (9).

1. Average speed in all cells remains at a constant value, i.e. $v_u^{i,j}(k) = v_{crit} \forall i, j, u, k$. v_{crit} also refers to the speed of the slower vehicle class. All vehicle classes travel with the same critical speed at the critical density [26]. Please note that this assumption is only made to design a multi-class lane-changing controller. We will later see in a simulation-based case study (section VI) that this assumption does not limit the performance of the proposed controller. Due to its robust feedback-based mechanism, the controller is able to improve traffic efficiency around a merging section.
2. Since speed remains at a constant value, we can also assume fixed passenger car equivalents.
3. Measurable inflows are constant, i.e. $d_u^{i,j}(k) = \underline{d}_u^{i,j} \forall i, j, u, k$. Please note that constant inflows would first enable us to define a linear time-invariant (LTI) system and then to derive a time-invariant feedback controller. However, we will allow these inflows to be time-varying according to real-time measurements, which we will explain later in detail (section II.B).

Under these assumptions, for two-vehicle classes, cars and trucks, (9) can be reformulated as follows:

$$\begin{aligned} \rho_{tot}^{i,j}(k+1) = & \frac{T}{L_i} (v_{crit}) \rho_{tot}^{i-1,j}(k) \\ & + \left(1 - \frac{T}{L_i} (v_{crit}) \right) \rho_{tot}^{i,j}(k) \\ & + \frac{T}{L_i} \left(\eta_c^{i,j-1} f_c^{i,j-1}(k) - \eta_c^{i,j} f_c^{i,j}(k) \right) \\ & + \frac{T}{L_i} \left(\eta_t^{i,j-1} f_t^{i,j-1}(k) - \eta_t^{i,j} f_t^{i,j}(k) \right) \\ & + \frac{T}{L_i} \left(\eta_c^{i,j} \underline{d}_c^{i,j} + \eta_t^{i,j} \underline{d}_t^{i,j} \right), \quad (10) \end{aligned}$$

where subscripts c and t denote cars and trucks, respectively.

Now the above system in (10) can be considered as an LTI system

$$\underline{x}(k+1) = A \underline{x}(k) + B \underline{u}(k) + \underline{d} \quad (11)$$

where

$$\underline{x} = \left[\rho_{tot}^{0,m_0} \dots \rho_{tot}^{0,M_0} \rho_{tot}^{1,m_1} \dots \rho_{tot}^{N,M_N} \right]^T \in \mathbb{R}^{\bar{H}}, \quad (12)$$

$$\underline{u} = \left[f_c^{0,m_0} \dots f_c^{0,M_0-1} f_c^{1,m_1} \dots f_c^{N,M_N-1} \right. \\ \left. f_t^{0,m_0} \dots f_t^{0,M_0-1} f_t^{1,m_1} \dots f_t^{N,M_N-1} \right]^T \in \mathbb{R}^{\bar{F}}, \quad (13)$$

$$\underline{d} = \left[\frac{T}{L_i} \left(\eta_c^{0,m_0} \underline{d}_c^{0,m_0} + \eta_t^{0,m_0} \underline{d}_t^{0,m_0} \right) \dots \right. \\ \frac{T}{L_i} \left(\eta_c^{0,M_0} \underline{d}_c^{0,M_0} + \eta_t^{0,M_0} \underline{d}_t^{0,M_0} \right) \\ \frac{T}{L_i} \left(\eta_c^{1,m_1} \underline{d}_c^{1,m_1} + \eta_t^{1,m_1} \underline{d}_t^{1,m_1} \right) \\ \left. \dots \frac{T}{L_i} \left(\eta_c^{N,M_N} \underline{d}_c^{N,M_N} + \eta_t^{N,M_N} \underline{d}_t^{N,M_N} \right) \right]^T \in \mathbb{R}^{\bar{H}}. \quad (14)$$

This LTI system in (11) can be used to formulate an optimal control problem that is aimed at maximizing traffic efficiency by balancing flows among lanes on a freeway. $A \in \mathbb{R}^{\bar{H} \times \bar{H}}$, composed of a_{rs} elements, represents the connection between pairs of subsequent cells connected by a longitudinal flow and $B \in \mathbb{R}^{\bar{H} \times \bar{F}}$, composed of b_{rs} elements, reflects the connection of adjacent cells connected by lateral flows. These elements are given by:

$$a_{rs} = \begin{cases} 1 - \frac{T}{L_i} (v_{crit}), & \text{if } r = s \text{ and } (i = N \text{ or } m_{i+1}) \\ & \leq j \leq M_{i+1}) \\ \frac{T}{L_i} (v_{crit}), & \text{if } r > H_0 \text{ and } s = r - M_{i-1} \\ & + m_i - 1 \\ 0, & \text{otherwise} \end{cases} \quad (15)$$

$$b_{rs} = \begin{cases} \eta_c^{i,j} \frac{T}{L_i}, & \text{if } j > m_i \text{ and } (s = r - i) \\ -\eta_c^{i,j} \frac{T}{L_i}, & \text{if } j < M_i \text{ and } (s = r - i + 1) \\ \eta_t^{i,j} \frac{T}{L_i}, & \text{if } j > m_i \text{ and } (s = r + \bar{H} - N - i) \\ -\eta_t^{i,j} \frac{T}{L_i}, & \text{if } j < M_i \text{ and } (s = r + \bar{H} - N - i + 1) \\ 0, & \text{otherwise} \end{cases} \quad (16)$$

where $r = H_{i-1} + j - m_i$.

B. Optimal Control Problem Formulation

The optimal control minimizes a cost function to steer a system to the desired state. The following quadratic cost function, over an infinite time horizon, has been defined:

$$\min J = \sum_k^\infty \left\{ \sum_{\hat{i}} \sum_{\hat{j}} \alpha^{\hat{i},\hat{j}} \left(\rho_{tot}^{\hat{i},\hat{j}}(k) - \hat{\rho}_{crit}^{\hat{i},\hat{j}} \right)^2 \right. \\ \left. + \sum_{i=0}^{N-1} \sum_{j=m_i}^{M_i-1} \sum_u \varphi_u^{i,j} f_u^{i,j}(k)^2 \right\}, \quad (17)$$

where (\hat{i}, \hat{j}) are the targeted cells; $\hat{\rho}_{crit}^{\hat{i},\hat{j}}$ is the desired set-point; $\alpha^{\hat{i},\hat{j}}$ is the weight associated with the targeted

cell (\hat{i}, \hat{j}) ; and $\varphi_u^{i,j}$ is the weight associated with the control actions for a vehicle class u at a cell (i, j) . The cost function aims to penalize the difference between selected cell densities and the corresponding pre-defined set points. In addition, it also penalizes excessive lane changes, thus maintaining small control inputs.

Equation (17) can be written in the matrix form as follows:

$$\min J = \sum_{k=0}^\infty \left\{ [C\underline{x}(k) - \hat{y}]^T Q [C\underline{x}(k) - \hat{y}] \right. \\ \left. + \underline{u}(k)^T R \underline{u}(k) \right\}, \quad (18)$$

where $Q = Q^T \geq 0$ and $R = \begin{bmatrix} \phi_c I_{\bar{F}/2} & 0_{\bar{F}/2} \\ 0_{\bar{F}/2} & \phi_t I_{\bar{F}/2} \end{bmatrix}$ are the weights associated with tracking and control actions, respectively. \hat{y} refers to a vector of set-points and is of dimension $\mathbb{R}^{\bar{Y}}$. C reflects the cells that are tracked. The parameters $\phi_c > 0$ and $\phi_t > 0$ penalize fluctuations of car and truck-specific lateral flows, respectively.

The matrix C is of dimension $\mathbb{R}^{\bar{Y} \times \bar{H}}$. Each row of matrix C contains a single element that corresponds to the cell that is tracked with the value of one, while the rest of the elements are equal to zero. Since, in this paper, we target only cells in section N , the matrix C can be written as follows:

$$C = \begin{bmatrix} 0_{\bar{Y} \times (\bar{H} - \bar{Y})} & I_{\bar{Y} \times \bar{Y}} \end{bmatrix}. \quad (19)$$

The problem defined in (18) is subject to the linear dynamics presented in (11). Assuming the system is stabilizable and detectable, we can solve this type of problem using a linear quadratic regulator. Since the stabilizability and detectability for such systems have been established in [13] and [14], the solution to the proposed optimal control problem can be given by the following linear feedback-feedforward control law:

$$\underline{u}^*(k) = -K\underline{x}(k) + \underline{u}_{ff}, \quad (20)$$

where

$$K = (R + B^T P B)^{-1} B^T P A, \quad (21)$$

$$P = C^T Q C + A^T P A - A^T P B (R + B^T P B)^{-1} B^T P A, \quad (22)$$

$$\underline{u}_{ff} = (R + B^T P B)^{-1} B^T F (C^T Q \hat{y} - P \underline{d}), \quad (23)$$

$$F = (I - (A - B K)^T)^{-1}. \quad (24)$$

The feedback gain matrix can be computed offline by solving the Riccati equation. For practical implementation, we may assume that external flows can be measured. In that case, the feed-forward term becomes time-varying. Now, we can rewrite (20) and (23) as follows:

$$\underline{u}^*(k) = -K\underline{x}(k) + \underline{u}_{ff}(k), \quad (25)$$

$$\underline{u}_{ff}(k) = \Phi - \psi \underline{d}(k), \quad (26)$$

where $\Phi = (R + B^T P B)^{-1} B^T F (C^T Q \hat{y})$ and $\psi = (R + B^T P B)^{-1} B^T F P$ may be calculated offline.

C. Transferring the Optimal LQR Control to a Real-World C-ITS-Based Multi-Class Lane-Changing Advisory System

The proposed feedback-feedforward control law, given by (25), can effectively be used to design a real-world C-ITS based lane-changing advisory system since the computation of control inputs depend on the feedback gain matrix K , the feedforward term comprising matrices Φ and Ψ , measurement of state variables and external flows arising from outside the boundary of the considered system. For practical applications, the computation of matrices K , Φ , and Ψ may be done once offline. Once we have these matrices, online computation is only limited to a few matrix-vector multiplications, as shown in (25) and (26). The measurement of state variables or density of each considered cell is required every time step in real-time. To produce these measurements, a traffic state estimator [27]–[32] can be embedded in the control loop.

The proposed lane-changing advisory system requires an exchange of information between the traffic control center and vehicles. Vehicles are required to have connectivity in order to facilitate this exchange. Before control inputs or lane-changing advice are sent to the vehicles, it is vital to know vehicles' position (i.e., lane and location) and type (e.g., cars or trucks). We might require roadside units (RSUs) to gather position and vehicle type data via V2I communications for a particular cell. These data would be processed at the traffic control center to know which vehicles are present in a specific cell. With this information, the traffic control center can then issue lane-changing advice to a selection of vehicles through I2V communications (e.g., via RSUs) to indicate whether they need to change lanes. In practice, the selection of vehicles may be based on their destinations known beforehand to improve the positive effects arising from the advisory system. This system only advises vehicles to change lanes as it does not force them to change lanes. However, any mismatch between the control inputs or advised lane changes and actual lane changes due to compliance rate may be balanced by the feedback nature of the proposed controller. Spontaneous lane changes might also arise and these may be reduced by issuing additional lane-keeping advice to drivers not selected earlier.

Lane-changing advice may be communicated to vehicles using an in-vehicle interface (e.g., smartphone application or vehicle's touchscreen) in the form of text or sound. A number of C-ITS real-world applications also prefer these modes of issuing advice to drivers [33], [34]. Fig. 2 shows a C-ITS-based multi-class lane-changing advisory framework for a merging section.

III. IMPLEMENTATION OF LANE-CHANGING ADVISORY SYSTEM IN A MICROSCOPIC TRAFFIC SIMULATOR

The proposed control strategy is tested using the microscopic traffic simulator OpenTrafficSim [35], which is a Java-based open-source software package. It combines IDM+ as the car-following model [36] and the lane-changing model with relaxation and synchronization (LMRS) as the lane-changing model [37]. We assume that there is no latency in V2I or I2V communication at the controller level. The proposed controller requires density measurements for all cells that are considered

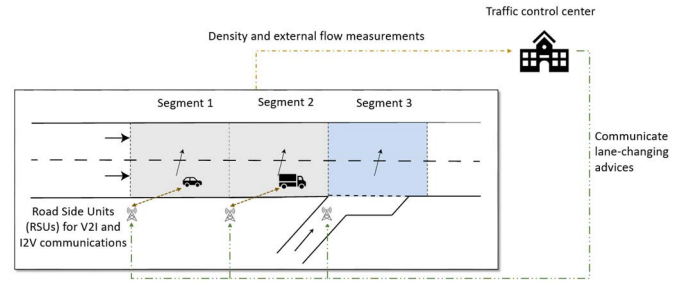


Fig. 2. C-ITS based multi-class lane-changing advisory framework.

for the lane-changing advisory system and external demand that arise from outside the system boundaries. To realize the control actions, we keep individual lists of vehicles (cars and trucks) present in those cells. Note that we keep an individual list for every such cell which is of interest to the lane-change controller. Since this is a dynamic list, it gets updated every time a vehicle enters or exits that cell. Depending on the control action, we randomly select the desired number (requested by the controller) of cars and trucks from the list for a specific cell. These vehicles (cars and trucks) are instructed to follow the lane-change advisory using the lane-changing model (LMRS). Please note that some of the vehicles may not be able to perform lane changes due to the logic of the lane-changing model; however, this limited compliance is balanced by the feedback nature of the proposed controller. Next, we present the LMRS model.

A. Lane-Changing Model

We have selected the Lane change model with Relaxation and Synchronization (LMRS) as our base model [37]. The LMRS is based on the desire of a vehicle to change lanes that comes from several motivations. The base LMRS model aggregates considered motivations as follows:

$$d^{y,z} = d_r^{y,z} + \theta_v^{y,z} (d_s^{y,z} + d_b^{y,z}), \quad (27)$$

where $d^{y,z}$ is the total/aggregated desire to change lanes. $d_r^{y,z}$, $d_s^{y,z}$, and $d_b^{y,z}$ refer to the desire for following a route, the desire to gain or maintain speed, and the desire to follow a keep-right policy, respectively. Here, $\theta_v^{y,z}$ denotes the weights associated with voluntary motivations. The desire toward voluntary motivations ($d_v^{y,z}$) comes from $d_s^{y,z}$ and $d_b^{y,z}$.

The value of the desire to change from lane y to lane z is $d^{y,z}$, and it ranges between -1 and 1, where only positive values influence a lane-changing decision. The positive range is divided into four areas ($0 < d_{\text{free}} < d_{\text{sync}} < d_{\text{coop}} < 1$) which determines the way a lane-change is performed. In the following, we discuss how a lane-changing is performed if the desire (d) falls in one of the four areas.

- 1) $d < d_{\text{free}}$: the desire is too small for a vehicle to perform a lane change.
- 2) $d_{\text{free}} \leq d < d_{\text{sync}}$: a vehicle performs a lane change if it is possible.
- 3) $d_{\text{sync}} \leq d < d_{\text{coop}}$: if the adjacent gap in the target lane is not feasible, a vehicle aligns its speed to that of the leader in the target lane.

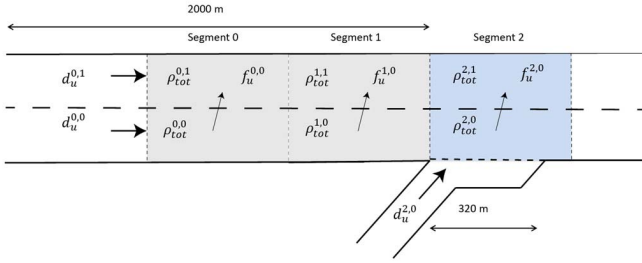


Fig. 3. 2-lane mainline carriageway with an on-ramp.

- 4) $d_{\text{coop}} \leq d$: the follower in the target lane adjusts its behavior to create a suitable gap to a lane-changing vehicle.

We extend this model to implement the LQR controller proposed in this paper.

B. Implementing the Lane-Changing Advisory System

The base LMRS model is essentially a linear-in-parameter formulation that can be extended to incorporate several other voluntary motivations. Consequently, we extend this base model to accommodate a lane change advisory framework in the following equation:

$$d^{y,z} = d_r^{y,z} + \theta_v^{y,z} (d_s^{y,z} + d_b^{y,z} + d_a^{y,z}), \quad (28)$$

where $d_a^{y,z}$ refers to an additional incentive that is triggered if a vehicle receives lane change advice from the control center. This incentive is formulated as follows:

$$d_a^{y,y-1} = \begin{cases} d_{\text{free}}, & \text{if a vehicle receives the lane} \\ & \text{change advice} \\ 0, & \text{otherwise} \end{cases} \quad (29)$$

$$d_a^{y,y+1} = 0, \quad (30)$$

where y , $y-1$, and $y+1$ refer to the current lane, left lane, and right lane in the direction of driving.

Once a vehicle gets the lane change advice, it has an additional desire d_{free} to move to its left lane. If the adjacent gap on the left lane is not suitable, the subject vehicle will continue in the current lane. Since we assume European driving conditions in our simulations, we expect vehicles to follow the keep-right policy. Therefore, we deactivate the subject vehicle's adherence to the keep-right policy ($d_b^{y,z}$) until it passes the merging section so that vehicle complies with the advisory issued by the traffic control center.

IV. EXPERIMENTAL SETUP

In this section, we describe the network, demand profile, and model parameters used for simulation, scenarios considered, and the performance indicators to assess the performance of the LQR control-based lane-changing advisory framework.

A. Study Area

We consider a merging section for the evaluation of the proposed multi-class lane change controller. The merging section (i.e., Ter Heijde) with a 2-lane mainline carriageway

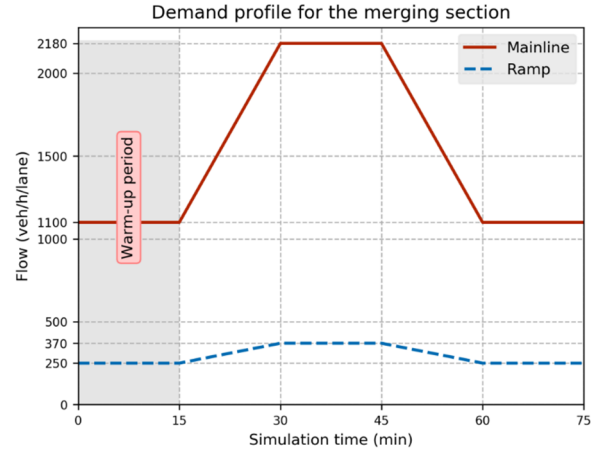


Fig. 4. Demand profile for the experimental setup.

is located on the A59 freeway in the Netherlands (see Fig. 3). The acceleration lane is 320 m long. The upstream segment of the considered merging section is 2 km long. We consider three segments, numbered as 0, 1, and 2 in Fig. 3, each 500 m long where vehicles will respond to lane change advisory issued by the control center. The nominal speed limit is 80 km/h for all those segments. This value is also the speed limit for trucks on freeways in the Netherlands.

B. Demand Profile

We consider a trapezoidal demand profile for mainline and ramp traffic (see Fig. 4). This trapezoidal demand is used to generate vehicles in the network. The generation time of vehicles in the network depends on randomly distributed generation time-headways. In this paper, we have assumed exponentially distributed headways. The share of trucks is 15% in the traffic mix. All simulations are conducted for 75 minutes of which the first 15 minutes are taken as the warm-up time. The purpose of warm-up time is to fill the network so that appropriate effects can be analyzed.

C. Simulation Model Parameters

Most of the simulation model parameters are equal to the default values which are calibrated for a freeway network located in the Netherlands by [37]. For trucks, we use the desired speed distribution (km/h) obtained from a web-based survey, i.e., $v_{\text{des,truck}} = N(84.14, 3.92)$. The lane-changing duration for truck drivers is obtained from a trajectory dataset [38], [39]. We use this dataset to obtain a normally distributed lane-changing duration (s) (i.e., $N(8.32, 2.19)$) for truck drivers. The simulation model parameters are tabulated in Table I.

D. Scenarios

We consider two scenarios to evaluate the performance of the LQR control-based lane-changing advisory framework.

- 1) No-control: In this case, vehicles are not issued lane change advisory.
- 2) LQR control: In this case, mainline vehicles are issued lane change advisory every 20 s. We assume that 100% of

TABLE I
SIMULATION MODEL PARAMETERS

Symbol	Value	Description
Car-following parameters		
a_{car}	1.25	Maximum (desired) car-following acceleration for cars (m/s^2)
a_{truck}	0.40	Maximum (desired) car-following acceleration for trucks (m/s^2)
b	2.09	Maximum comfortable car-following deceleration (m/s^2)
b_0	0.50	Maximum adjustment deceleration (m/s^2)
b_{crit}	3.50	Maximum critical deceleration (m/s^2)
f_{speed}	1.00	The speed limit adherence factor for cars and trucks
s_0	3.00	Car-following stopping distance (m)
T_{max}	1.20	Maximum car-following headway (s)
T_r	0.50	Reaction time (s)
$v_{des, car}$	$N(123.7, 12)$	Desired (maximum) speed for cars (km/h)
$v_{des, truck}$	$N(84.14, 3.92)$	Desired (maximum) speed for trucks (km/h)
l_{car}	4.00	Length of cars (m)
l_{truck}	15.00	Length of trucks (m)
Lane-changing parameters		
d_{free}	0.365	Free lane change desire threshold
d_{sync}	0.577	Synchronized lane change desire threshold
d_{coop}	0.788	Cooperative lane change desire threshold
T_{min}	0.56	Minimum car-following headway (s)
τ	25	Headway relaxation time (s)
v_{cong}	60	Speed threshold below which traffic is considered congested (km/h)
v_{gain}	50	Anticipation speed difference at full lane change desired (km/h)
x_0	295	Look-ahead distance (m)
t_0	43	Look-ahead time for mandatory lane changes (s)
$t_{ic,car}$	3	Lane change duration for passenger cars (s)
$t_{ic,truck}$	$N(8.32, 2.19)$	Lane change duration for trucks (s)

vehicles present in the traffic mix are connected vehicles that are able to receive the advisory. For cars, we use a pce value of 1.0. For trucks, we use a pce value of 1.61 which is taken from [26] where pce values are calibrated using a trajectory dataset.

E. Performance Indicator

We consider the Total Time Spent in the system (TTS in veh.h) as the performance indicator to evaluate the performance of the proposed controller. We do not take warm-up time into account to compute the TTS. TTS can be mathematically expressed as:

$$TTS = \sum_{i=1}^N (t_{exit}^i - t_{enter}^i), \quad (31)$$

where t_{enter}^i and t_{exit}^i refer to the time instant a vehicle i enters and exits the network, respectively. N denotes the total number of vehicles that have passed through the merging section in the simulation period. TTS can be further divided into the Total Travel Time for mainline vehicles (TTT) and the Total Waiting Time for ramp vehicles (TWT) to gain insight into how the proposed controller affects their efficiency to pass through a merging section.

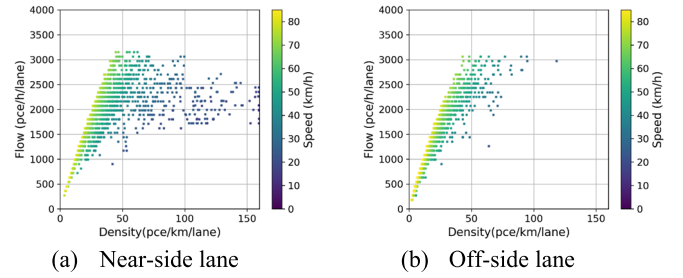


Fig. 5. Fundamental diagrams for (a) near-side; and (b) off-side lanes for 10 different simulation runs conducted for the no-control scenario.

V. SELECTION OF LQR CONTROLLER'S PARAMETERS

This section focuses on the selection of the LQR controller's parameters. First, we present an analysis of the choice of set points. Lastly, we present a response-surface-based method to optimally select the weights of Q and R matrices.

A. Reference Values of Set-Points and Weights Associated With Q and R Matrices

For the sensitivity analysis presented in this section, we use reference values for the set-points, and weights of Q and R matrices. For the set points, we use the critical density of the lane as the reference value. To compute the critical density, we generate fundamental diagrams (see Fig. 5) for the no-control case using data collected from 10 simulation runs. We use 40 pce/km/lane as the critical density for both the near-side and off-side lanes. With the given reference values of the set-points and desire threshold, we use a trial-and-error approach to select the reference weights for the Q and R matrices as:

$$Q = 10^2 I_2, \quad (32)$$

$$R = 10^1 I_6, \quad (33)$$

where $\phi_c = \phi_t = 10^1$.

B. Selection of Set-Points (\hat{y})

To assess the impact of set-points on the performance of the LQR controller, we select the reference values of the desire threshold and weights of the Q and R matrices. The critical density for each lane is computed as 40 pce/km/lane for which the system is able to maintain free-flow conditions. This value is taken as a starting point to define set points. We further increase this value in steps up to 45 pce/km/lane. Fig. 6 shows the performance of the LQR controller for the considered values of set-points with fixed Q and R matrices for 10 simulation runs. It can be observed that the LQR controller results in the best performance in terms of TTS of the system for the value of 41 pce/km/lane. We use this value as set points for our experiments.

C. Selection of Weighting Matrices (Q and R)

Now, we analyze the impact of weighting matrices (Q and R) on the performance of the LQR controller. The tuning of Q and R matrices presents a trade-off between tracking precision and the system's stability. In this section, we present a response-surface-based approach to select optimal weighting

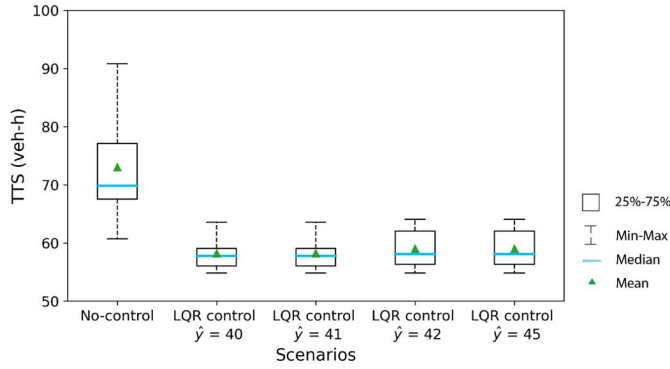


Fig. 6. Influence of set-points (\hat{y}) on the performance of the LQR controller for 10 simulation runs.

matrices of the LQR controller. This technique maps the impact of design variables on the processes. The technique can be separated into the following three stages [40].

- 1) selection of design variables,
- 2) selection of experimental design and model fitting, and
- 3) visualization of response surface and determination of optimal design parameters.

Next, we describe these steps in the detail.

1) *Selection of Design Variables*: Our design variables are the weighting matrices of the LQR controller. We consider that Q and R matrices are diagonal in nature and they can be expressed as follows for our test case:

$$Q = 10^{\theta_1} I_2, \quad (34)$$

$$R = 10^{\theta_2} I_6. \quad (35)$$

where θ_1 and θ_2 refer to the parameters intending to change the weights of the Q and R matrices. Here, we assume that $\phi_c = \phi_t = 10^{\theta_2}$.

2) *Selection of Experimental Design and Model Fitting*: We use the Latin hypercube sampling method to generate a response surface with input variables of θ_1 and θ_2 [41]. The design range of input variables is considered as $-5 \leq \theta_1$, $\theta_2 \leq 5$. We use a two-step approach to produce the response surface. First, we use 35 design points in the above design range of input variables. Then, we further focus on a smaller area ($0 \leq \theta_1 \leq 5$ and $-2 \leq \theta_2 \leq 5$) where there might be a higher possibility for a minimum to occur. In this area, we sample additional 30 design points. Overall, we use 65 design points to produce the response surface. The dependent variable is considered as TTS, which is obtained as the average TTS from 10 simulation runs. We use Lowess smoothing or locally weighted linear regression-based surface fitting procedure to convert the discrete design space to a continuous one (see Fig. 7). Lowess smoothing is a non-parametric technique to fit surfaces [42]. The fitting process is estimated locally by using the weighted neighborhood points with their distance to the observed point. The proportion of neighborhood points in the estimation depends on the span size. After analyzing root mean square error (RMSE), we choose a span size of 0.25 (RMSE = 2.53). The produced fit has $R^2 = 0.8990$ and adjusted $R^2 = 0.8843$ which indicates that 89.90% of the total variation can be explained by the fitted model.

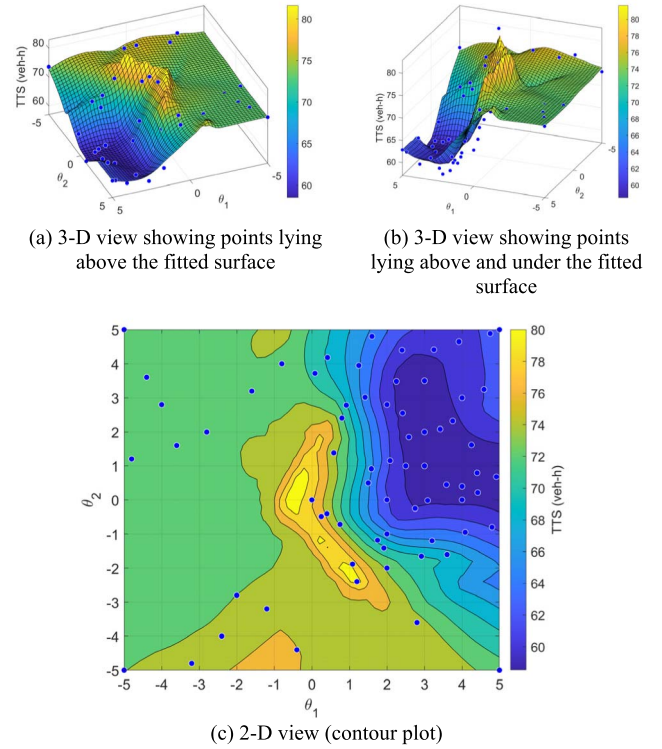


Fig. 7. Response surface generated by varying the weights of Q and R matrices (color bar shows TTS values where low TTS values are highlighted in blue).

3) *Visualization of Response Surface and Determination of Optimal Design Parameters*: The response surface and the contour plot show that multiple combinations of θ_1 and θ_2 yield similar performance. In the dark blue region (see Fig. 7), the LQR controller is little sensitive to the changes in the values of θ_1 and θ_2 . In order to guarantee a stable LQR controller, the values of θ_1 and θ_2 should be selected from the dark blue region shown in the contour plot.

Next, we present and discuss simulation results in order to discuss the performance of the LQR controller at a merging section.

VI. RESULTS AND DISCUSSION

In the scope of this work, we target only cells in segment 2 of the merging section. We use fundamental diagrams to find the set points for the LQR controller. For both the near-side and off-side lanes at segment 2, we use 41 pce/km/lane as set-points that is closer to their critical density values. The weights of the LQR controller are obtained from the contour plot. Q and R matrices are selected as $10^3 I_2$ and $10^1 I_6$, respectively. The LQR controller gains are computed offline and simulations are conducted using those values. In the following, we present a quantitative and qualitative evaluation of the performance of the LQR controller.

A. Quantitative Evaluation of the Performance of the LQR Controller

The performance of the LQR controller, in terms of TTS, is evaluated over 10 simulation runs (see Fig. 8 (a)). We obtain a TTS value of 73.04 veh-h for the no-control case. In comparison to the no-control case, we obtain an average TTS

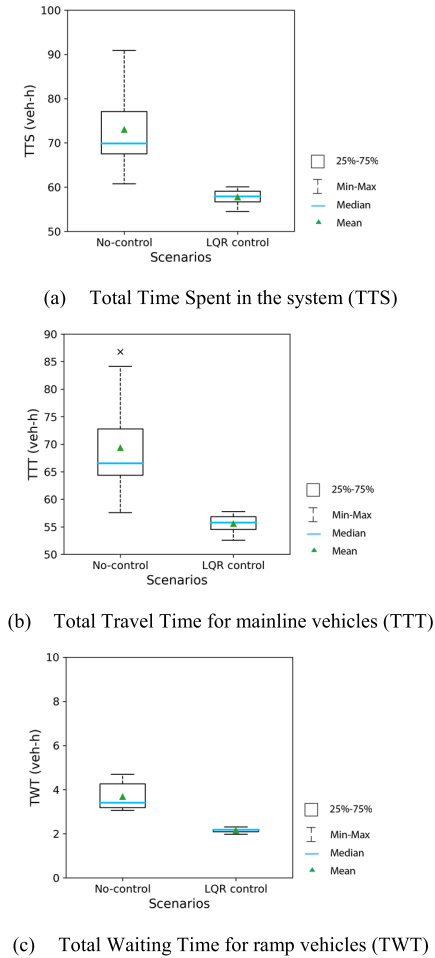


Fig. 8. Comparison between no-control and LQR control scenario for system (TTS), mainline (TTT) and ramp (TWT) vehicles.

equal to 57.74 veh·h in the controlled case which is around 21% improvement (t-statistic = 4.63, p-value = 0.001). The variance is significantly reduced in the control scenario thus indicating the consistent performance of the proposed lane-changing advisory system. Next, we discuss how the LQR controller affects the travel times of mainline and ramp vehicles.

Fig. 8 (b) presents the performance of the LQR controller in terms of TTT over 10 simulation runs. In the no-control case, an average TTT is computed to be 69.36 veh·h. When the LQR controller is applied, the average TTT is obtained as 55.59 veh·h which implies 19.85% improvement (t-statistic = 4.38, p-value = 0.001) than the no control case. The performance of the LQR controller in terms of TWT over 10 simulation runs is shown in Fig. 8 (c). For ramp vehicles, an average TWT is computed to be 3.68 veh·h for the no-control case. The LQR controller is able to improve the average TWT by 41.55% (t-statistic = 7.81, p-value = $1.77e-5$) as the average TWT gets reduced to 2.15 veh·h.

Overall, the LQR controller is able to improve traffic efficiency for both mainline and ramp vehicles thus showing significant improvement at the system level. Next, we present a qualitative evaluation concerning the performance of the LQR controller.

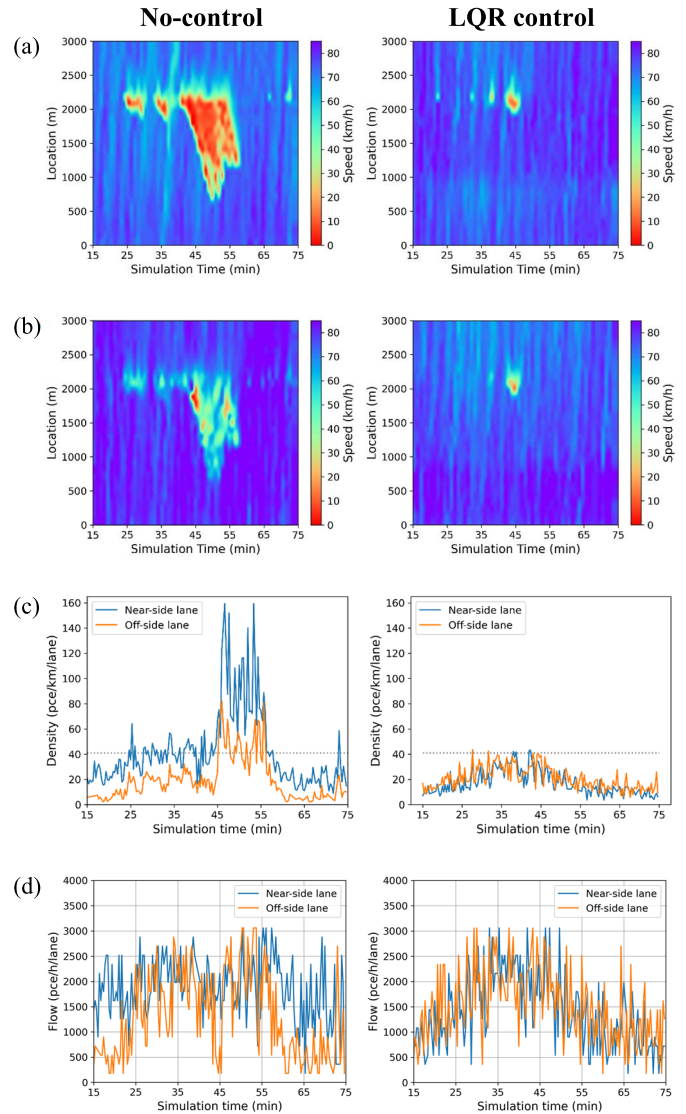


Fig. 9. Qualitative assessment of the LQR controller's performance for an average scenario (a) speed contour plots for the near-side lane (b) speed contour plots for the off-side lane, (c) density profile for near-side and off-side lanes at segment 2, and (d) outflow profile for near-side and off-side lanes at segment 2.

B. Qualitative Evaluation of the Performance of the LQR Controller

In Fig. 9, we present an evaluation of the performance of the LQR controller for an average scenario in terms of speed-contour plots, density profile, and outflow profile. By looking at speed-contour plots, we can observe that the LQR controller is able to suppress shockwaves in the system. Furthermore, we can observe that density values for both near-side and off-side lanes lie around set-points chosen for the LQR-control case compared to the no-control case. In the LQR control case, we observe that the distribution of traffic is more balanced since we observe similar density profiles for both lanes at segment 2. Fig. 9 (d) shows the observed outflow at the merging section. In the no-control scenario, the traffic flow on the nearside lane breaks down at around 2880 pce/h/lane before reaching its capacity. This also triggers a breakdown in the offside lane, before reaching its capacity, where for some time

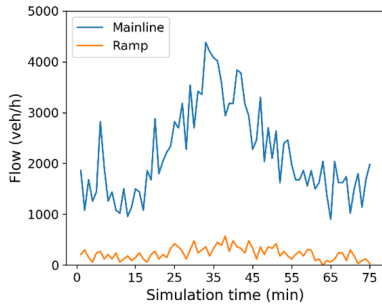


Fig. 10. Demand profile generated for an average scenario under the LQR control case.

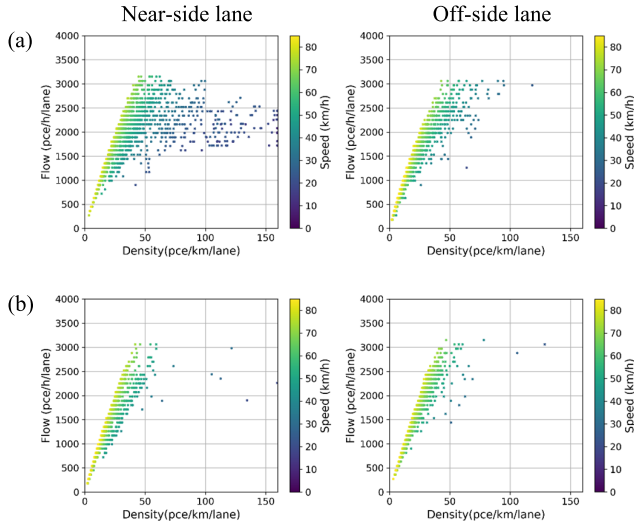


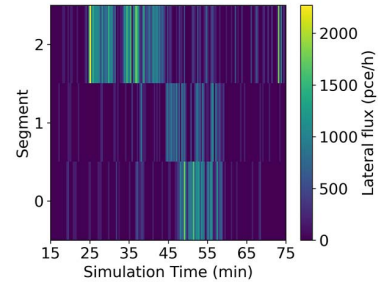
Fig. 11. Lane-specific fundamental diagrams at segment 2 generated for (a) no-control and (b) LQR control scenario using data collected from 10 simulation runs.

windows we observe outflow even lower than 500 pce/h/lane. Whereas in the LQR control scenario, we observe that outflow is reaching higher values (i.e., 3060 pce/h/lane) for a longer period of time without incurring traffic breakdown.

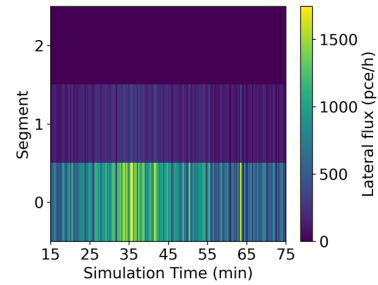
Interestingly, we observe a dip in density and outflow between 35-45 minutes in the LQR control scenario. This is attributed to the demand profile presented in Fig. 10. To generate this demand profile, we have placed loop-detectors at the entrance of the mainline and ramp. Fig. 10 shows a similar dip in traffic demand between 35-45 minutes. The results suggest that the buildup of density on the near-side and off-side lane follows the traffic pattern under the LQR control scenario. The LQR controller recognizes the randomly distributed demand (or generation of vehicles in the network) and effectively balances the distribution of traffic on both lanes.

We also analyze the performance of the LQR controller by comparing the lane-specific fundamental diagrams generated for segment 2 from 10 simulation runs. Fig. 11 shows that the LQR controller can improve the traffic efficiency around the merging section and successfully prevents the breakdown of traffic.

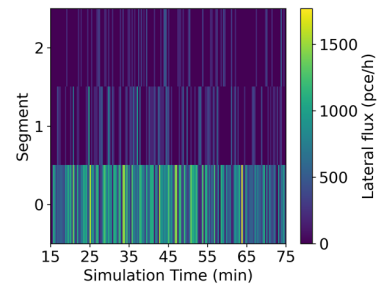
Now we will look at the distribution of lateral flux, from left to right side, over considered three segments around the merging section. Fig. 12 (a) shows that a high amount of lane-changing activity at segment 2, which is close to the



(a) Lateral flux in the no-control scenario



(b) Lateral flux advised by the LQR controller



(c) Lateral flux realized in the LQR control scenario

Fig. 12. Contour plots of lateral flux in (a) the no-control scenario, (b) advised LQR control scenario, and (c) the realized LQR control scenario.

merging section, for the no-control scenario. It appears that vehicles react to the congestion only if they can witness any impact within their visible range or look-ahead distance. Since the congestion starts to build up at the near-side lane after 35 minutes, the lane-changing activity starts to shift upstream to segments 0 and 1. Fig. 12 (b) presents the lateral flux advised by the LQR controller. We observe that the LQR controller emphasizes proactive lane-changing and advises vehicles to consider lane-changing ahead of reaching close to the merging section. In Fig. 12 (c), we present the realized lateral flux in the LQR control scenario. This realization depends on the gap-seeking behavior of vehicles governed by the LMRS model. Lateral flux is distributed in a way so that vehicles perform most of the lane-changing activity upstream at segment 0. We do note a few lane changes at segment 2 which can be attributed to the selection of vehicles and their ability to seek gaps.

VII. CONCLUSION AND FUTURE WORK

This paper develops a multi-class lane-changing advisory system based on a linear quadratic regulator. This system uses V2I and I2V communications and can be viewed as a cooperative intelligent transportation systems application.

We evaluate the performance of this system using microscopic simulation. The results indicate that this system can improve traffic efficiency around a merging section. Moreover, it brings substantial travel time benefits for both mainline and ramp vehicles. The findings will be of interest to traffic management agencies and logistics companies which are especially concerned about the travel time reliability of freight corridors. In the future, the effectiveness of the proposed framework can be evaluated for a scenario that includes truck platoons along with passenger cars and trucks. In addition, a promising research direction can be to include automated vehicles in the traffic mix. Furthermore, the lane-changing controller can be integrated into other local control strategies such as ramp metering.

ACKNOWLEDGMENT

The authors would like to thank Dr. Wouter Schakel from TU Delft for his help with simulation experiments.

REFERENCES

- [1] M. J. Cassidy and R. L. Bertini, "Some traffic features at freeway bottlenecks," *Transp. Res. B, Methodol.*, vol. 33, no. 1, pp. 25–42, Feb. 1999, doi: [10.1016/S0191-2615\(98\)00023-X](https://doi.org/10.1016/S0191-2615(98)00023-X).
- [2] M. J. Cassidy and J. Rudjanakanoknad, "Increasing the capacity of an isolated merge by metering its on-ramp," *Transp. Res. B, Methodol.*, vol. 39, no. 10, pp. 896–913, 2005, doi: [10.1016/j.trb.2004.12.001](https://doi.org/10.1016/j.trb.2004.12.001).
- [3] V. L. Knoop, A. Duret, C. Buisson, and B. van Arem, "Lane distribution of traffic near merging zones influence of variable speed limits," in *Proc. 13th Int. IEEE Conf. Intell. Transp. Syst.*, Sep. 2010, pp. 485–490, doi: [10.1109/ITSC.2010.5625034](https://doi.org/10.1109/ITSC.2010.5625034).
- [4] N. Wu, "Equilibrium of lane flow distribution on motorways," *Transp. Res. Record, J. Transp. Res. Board*, vol. 1965, no. 1, pp. 48–59, Jan. 2006, doi: [10.1177/0361198106196500106](https://doi.org/10.1177/0361198106196500106).
- [5] M. R. Amin and J. H. Banks, "Variation in freeway lane use patterns with volume, time of day, and location," *Transp. Res. Rec., J. Transp. Res. Board*, vol. 1934, no. 1, pp. 132–139, Jan. 2005, doi: [10.1177/0361198105193400114](https://doi.org/10.1177/0361198105193400114).
- [6] K. Sjoberg *et al.*, "Cooperative intelligent transport systems in Europe: Current deployment status and outlook," *IEEE Veh. Technol. Mag.*, vol. 12, no. 2, pp. 89–97, Jun. 2017, doi: [10.1109/MVT.2017.2670018](https://doi.org/10.1109/MVT.2017.2670018).
- [7] Y. Zhang and P. A. Ioannou, "Combined variable speed limit and lane change control for highway traffic," *IEEE Trans. Intell. Transp. Syst.*, vol. 18, no. 7, pp. 1812–1823, Jul. 2017, doi: [10.1109/TITS.2016.2616493](https://doi.org/10.1109/TITS.2016.2616493).
- [8] W. J. Schakel and B. van Arem, "Improving traffic flow efficiency by in-car advice on lane, speed, and headway," *IEEE Trans. Intell. Transp. Syst.*, vol. 15, no. 4, pp. 1597–1606, Aug. 2014, doi: [10.1109/TITS.2014.2303577](https://doi.org/10.1109/TITS.2014.2303577).
- [9] M. Ramezani and E. Ye, "Lane density optimisation of automated vehicles for highway congestion control," *Transportmetrica B, Transp. Dyn.*, vol. 7, no. 1, pp. 1096–1116, Dec. 2019, doi: [10.1080/21680566.2019.1568925](https://doi.org/10.1080/21680566.2019.1568925).
- [10] C. Zhang, N. R. Sabar, E. Chung, A. Bhaskar, and X. Guo, "Optimisation of lane-changing advisory at the motorway lane drop bottleneck," *Transp. Res. C, Emerg. Technol.*, vol. 106, pp. 303–316, Sep. 2019, doi: [10.1016/j.trc.2019.07.016](https://doi.org/10.1016/j.trc.2019.07.016).
- [11] H. H. S. N. Subraveti, V. L. Knoop, and B. van Arem, "Improving traffic flow efficiency at motorway lane drops by influencing lateral flows," *Transp. Res. Rec., J. Transp. Res. Board*, vol. 2674, no. 11, pp. 367–378, Nov. 2020, doi: [10.1177/0361198120948055](https://doi.org/10.1177/0361198120948055).
- [12] V. Markantonakis, D. I. Skoufoulas, I. Papamichail, and M. Papageorgiou, "Integrated traffic control for freeways using variable speed limits and lane change control actions," *Transp. Res. Rec., J. Transp. Res. Board*, vol. 2673, no. 9, pp. 602–613, Sep. 2019, doi: [10.1177/0361198119846476](https://doi.org/10.1177/0361198119846476).
- [13] C. Roncoli, N. Bekiaris-Liberis, and M. Papageorgiou, "Optimal lane-changing control at motorway bottlenecks," in *Proc. 19th IEEE Int. Conf. Intell. Transp. Syst. (ITSC)*, Nov. 2016, pp. 1785–1791, doi: [10.1109/ITSC.2016.7795800](https://doi.org/10.1109/ITSC.2016.7795800).
- [14] C. Roncoli, N. Bekiaris-Liberis, and M. Papageorgiou, "Lane-changing feedback control for efficient lane assignment at motorway bottlenecks," *Transp. Res. Rec., J. Transp. Res. Board*, vol. 2625, no. 1, pp. 20–31, Jan. 2017.
- [15] F. Tajdari, C. Roncoli, N. Bekiaris-Liberis, and M. Papageorgiou, "Integrated ramp metering and lane-changing feedback control at motorway bottlenecks," in *Proc. 18th Eur. Control Conf. (ECC)*, Jun. 2019, pp. 3179–3184.
- [16] F. Tajdari, C. Roncoli, and M. Papageorgiou, "Feedback-based ramp metering and lane-changing control with connected and automated vehicles," *IEEE Trans. Intell. Transp. Syst.*, early access, Sep. 16, 2020, doi: [10.1109/TITS.2020.3018873](https://doi.org/10.1109/TITS.2020.3018873).
- [17] J. W. C. van Lint, S. P. Hoogendoorn, and M. Schreuder, "Fastlane: New multiclass first-order traffic flow model," *Transp. Res. Rec., J. Transp. Res. Board*, vol. 2088, no. 1, pp. 177–187, Jan. 2008, doi: [10.3141/2088-19](https://doi.org/10.3141/2088-19).
- [18] M. A. Johnson and M. J. Grimble, "Recent trends in linear optimal quadratic multivariable control system design," *IEE Proc. D, Control Theory Appl.*, vol. 134, no. 1, pp. 53–71, Jan. 1987, doi: [10.1049/ip-d.1987.0012](https://doi.org/10.1049/ip-d.1987.0012).
- [19] M. Saif, "Optimal linear regulator pole-placement by weight selection," *Int. J. Control*, vol. 50, no. 1, pp. 399–414, Jul. 1989, doi: [10.1080/00207178908953369](https://doi.org/10.1080/00207178908953369).
- [20] M. Habib, F. Khoucha, and A. Harrag, "GA-based robust LQR controller for interleaved boost DC–DC converter improving fuel cell voltage regulation," *Electr. Power Syst. Res.*, vol. 152, pp. 438–456, Nov. 2017, doi: [10.1016/j.epsr.2017.08.004](https://doi.org/10.1016/j.epsr.2017.08.004).
- [21] S. Das, I. Pan, K. Halder, S. Das, and A. Gupta, "LQR based improved discrete PID controller design via optimum selection of weighting matrices using fractional order integral performance index," *Appl. Math. Model.*, vol. 37, no. 6, pp. 4253–4268, Mar. 2013, doi: [10.1016/j.apm.2012.09.022](https://doi.org/10.1016/j.apm.2012.09.022).
- [22] K. Hassani and W.-S. Lee, "Multi-objective design of state feedback controllers using reinforced quantum-behaved particle swarm optimization," *Appl. Soft Comput.*, vol. 41, pp. 66–76, Apr. 2016, doi: [10.1016/j.asoc.2015.12.024](https://doi.org/10.1016/j.asoc.2015.12.024).
- [23] L. Liang, J. Yuan, S. Zhang, and P. Zhao, "Design a software real-time operation platform for wave piercing catamarans motion control using linear quadratic regulator based genetic algorithm," *PLoS ONE*, vol. 13, no. 4, Apr. 2018, Art. no. e0196107, doi: [10.1371/journal.pone.0196107](https://doi.org/10.1371/journal.pone.0196107).
- [24] R. H. Myers, Y. Kim, and K. L. Griffiths, "Response surface methods and the use of noise variables," *J. Quality Technol.*, vol. 29, no. 4, pp. 429–440, Oct. 1997, doi: [10.1080/00224065.1997.11979794](https://doi.org/10.1080/00224065.1997.11979794).
- [25] E. R. Ziegel, "Response surfaces: Designs and analyses," *Technometrics*, vol. 39, no. 3, p. 342, Aug. 1997, doi: [10.1080/00401706.1997.10485140](https://doi.org/10.1080/00401706.1997.10485140).
- [26] T. Schreiter, "Vehicle-class specific control of freeway traffic," Ph.D. dissertation, Transp. Planning, Delft Univ. Technol., Delft, The Netherlands, 2013, doi: [10.4233/uuid:e147786f-6658-496c-9fa5-d2e19e875fe2](https://doi.org/10.4233/uuid:e147786f-6658-496c-9fa5-d2e19e875fe2).
- [27] J. C. Herrera and A. M. Bayen, "Incorporation of Lagrangian measurements in freeway traffic state estimation," *Transp. Res. B, Methodol.*, vol. 44, no. 4, pp. 460–481, May 2010, doi: [10.1016/j.trb.2009.10.005](https://doi.org/10.1016/j.trb.2009.10.005).
- [28] T. Seo, T. Kusakabe, and Y. Asakura, "Estimation of flow and density using probe vehicles with spacing measurement equipment," *Transp. Res. C, Emerg. Technol.*, vol. 53, no. 6, pp. 134–150, 2015, doi: [10.1016/j.trc.2015.01.033](https://doi.org/10.1016/j.trc.2015.01.033).
- [29] N. Bekiaris-Liberis, C. Roncoli, and M. Papageorgiou, "Highway traffic state estimation per lane in the presence of connected vehicles," *Transp. Res. B, Methodol.*, vol. 106, pp. 1–28, Dec. 2017, doi: [10.1016/j.trb.2017.11.001](https://doi.org/10.1016/j.trb.2017.11.001).
- [30] S. Papadopoulou, C. Roncoli, N. Bekiaris-Liberis, I. Papamichail, and M. Papageorgiou, "Microscopic simulation-based validation of a per-lane traffic state estimation scheme for highways with connected vehicles," *Transp. Res. C, Emerg. Technol.*, vol. 86, pp. 441–452, Jan. 2018, doi: [10.1016/j.trc.2017.11.012](https://doi.org/10.1016/j.trc.2017.11.012).
- [31] Y. Yuan, J. W. C. van Lint, R. E. Wilson, F. van Wageningen-Kessels, and S. P. Hoogendoorn, "Real-time Lagrangian traffic state estimator for freeways," *IEEE Trans. Intell. Transp. Syst.*, vol. 13, no. 1, pp. 59–70, Mar. 2012, doi: [10.1109/TITS.2011.2178837](https://doi.org/10.1109/TITS.2011.2178837).
- [32] Y. Yuan, H. V. Lint, F. V. Wageningen-Kessels, and S. Hoogendoorn, "Network-wide traffic state estimation using loop detector and floating car data," *J. Intell. Transp. Syst.*, vol. 18, no. 1, pp. 41–50, 2014, doi: [10.1080/15472450.2013.773225](https://doi.org/10.1080/15472450.2013.773225).
- [33] M. Fukushima, "The latest trend of v2x driver assistance systems in Japan," *Comput. Netw.*, vol. 55, no. 14, pp. 3134–3141, Oct. 2011, doi: [10.1016/j.comnet.2011.03.012](https://doi.org/10.1016/j.comnet.2011.03.012).

- [34] F. Kanazawa, H. Kanoshima, K. Sakai, and K. Suzuki, "Field operational tests of smartway in Japan," *IATSS Res.*, vol. 34, no. 1, pp. 31–34, Jul. 2010, doi: [10.1016/j.iatssr.2010.07.001](https://doi.org/10.1016/j.iatssr.2010.07.001).
- [35] H. van Lint, W. Schakel, G. Tamminga, P. Knoppers, and A. Verbraeck, "Getting the human factor into traffic flow models: New open-source design to simulate next generation of traffic operations," *Transp. Res. Rec., J. Transp. Res. Board*, vol. 2561, no. 1, pp. 25–33, Jan. 2016, doi: [10.3141/2561-04](https://doi.org/10.3141/2561-04).
- [36] W. J. Schakel, B. van Arem, and B. D. Netten, "Effects of cooperative adaptive cruise control on traffic flow stability," in *Proc. 13th Int. IEEE Conf. Intell. Transp. Syst.*, Sep. 2010, pp. 759–764, doi: [10.1109/ITSC.2010.5625133](https://doi.org/10.1109/ITSC.2010.5625133).
- [37] W. J. Schakel, V. L. Knoop, and B. V. Arem, "Integrated lane change model with relaxation and synchronization," *Transp. Res. Rec.*, vol. 2316, no. 1, pp. 47–57, 2012, doi: [10.3141/2316-06](https://doi.org/10.3141/2316-06).
- [38] A. van Beinum, "Motorway turbulence—Empirical trajectory data," 4TU.ResearchData, Jun. 14, 2018, doi: [10.4121/uuid:6be1aef4-0803-4ce2-91b2-caaa7982abcd](https://doi.org/10.4121/uuid:6be1aef4-0803-4ce2-91b2-caaa7982abcd).
- [39] A. van Beinum, H. Farah, F. Wegman, and S. Hoogendoorn, "Driving behaviour at motorway ramps and weaving segments based on empirical trajectory data," *Transp. Res. C, Emerg. Technol.*, vol. 92, pp. 426–441, Jul. 2018, doi: [10.1016/j.trc.2018.05.018](https://doi.org/10.1016/j.trc.2018.05.018).
- [40] D. Bař and I. H. Boyacı, "Modeling and optimization I: Usability of response surface methodology," *J. Food Eng.*, vol. 78, no. 3, pp. 836–845, Feb. 2007, doi: [10.1016/j.jfoodeng.2005.11.024](https://doi.org/10.1016/j.jfoodeng.2005.11.024).
- [41] M. D. McKay, R. J. Beckman, and W. J. Conover, "A comparison of three methods for selecting values of input variables in the analysis of output from a computer code," *Technometrics*, vol. 21, no. 2, pp. 239–245, 1979, doi: [10.2307/1268522](https://doi.org/10.2307/1268522).
- [42] W. S. Cleveland and S. J. Devlin, "Locally weighted regression: An approach to regression analysis by local fitting," *Publications Amer. Statist. Assoc.*, vol. 83, no. 403, pp. 596–610, 1988, doi: [10.1080/01621459.1988.10478639](https://doi.org/10.1080/01621459.1988.10478639).



Salil Sharma received the B.Tech. degree in civil engineering from IIT Guwahati in 2010 and the M.Sc. degree in transportation systems from the Technical University of Munich, Germany, in 2016. He is currently pursuing the Ph.D. degree in transportation engineering with the Delft University of Technology, The Netherlands. His research interests include traffic flow theory, traffic management and control, cooperative and intelligent transportation systems, and transportation and freight data analytics.



Ioannis Papamichail received the Dipl.Eng. degree in chemical engineering from the National Technical University of Athens in 1998 and the M.Sc. degree in process systems engineering and the Ph.D. degree in chemical engineering from Imperial College London in 1999 and 2002, respectively.

From 1999 to 2002, he was a Research Assistant with the Center for Process Systems Engineering, Imperial College London. He joined the Technical University of Crete, Chania, Greece, in 2004, and has served, since then, at all academic ranks.

In 2010, he was a Visiting Scholar with the University of California at Berkeley, CA, USA. He is currently the Director of the Dynamic Systems and Simulation Laboratory, Technical University of Crete. He is the author of several technical papers in scientific journals and conference proceedings. His main research interests include automatic control and optimization theory and applications to traffic and transportation systems.

Dr. Papamichail received the 1998 Eugenidi Foundation Scholarship for Postgraduate Studies and the 2010 Transition to Practice Award from the IEEE Control Systems Society. He is also an Associate Editor of *IEEE TRANSACTIONS ON INTELLIGENT TRANSPORTATION SYSTEMS* and a Member of the Editorial Advisory Board for *Transportation Research—C: Emerging Technologies*.



Ali Nadi received the B.Sc. degree in civil engineering from the Arak University in 2011, and the M.Sc. degree in transportation engineering from the K. N. Toosi University of Technology in 2014. He is currently pursuing the Ph.D. degree in transportation with the Department of Transport and Planning, Faculty of Civil Engineering and Geosciences, Delft University of Technology (TU Delft), The Netherlands. He is also an Active Member of the Freight and Logistics Laboratory and the Delft Integrated Traffic and Travel Laboratory (DiTTLab, <https://dittlab.tudelft.nl>) and has hands-on experience in developing AI-based multi-class traffic models. He is also the Organizer of a series of freight and logistics webinars at TU Delft for the Freight Transport and Logistics Community. He is working on developing methods for integrative modeling of logistics and traffic systems using advanced data-driven and optimization techniques. His areas of expertise also include the integration of AI with operational research and theory-driven methods to model and control demand and supply interactions in both mobility and logistics systems.



Hans van Lint is currently a Full Professor of traffic simulation and computing with the Transport and Planning (T&P) Department, Faculty of Civil Engineering and Geosciences, and the Director of the Data Analytics and Simulation Laboratory (dittlab.tudelft.nl), Delft University of Technology. His research focuses on multi-scale estimation, prediction, and simulation of traffic supply and demand on large transport networks using an interdisciplinary mix of traffic flow theory, AI, and computer science.

In the last few years, he worked with his team for example on new OD estimation methods, traffic state estimation and prediction, and data-driven methods to unravel large-scale network dynamics and—at the other end of the spectrum—on new microscopic models for driving behavior that include human factors. He has (co)authored more than 70 articles in peer-reviewed international journals, supervise(s/d) 21 Ph.D. students, and served as an external examiner in Ph.D. committees for more than 30 other Ph.D. students in The Netherlands and abroad. He is on the Editorial Board of *Transportation Research—C: Emerging Technologies* and *IEEE TRANSACTIONS ON INTELLIGENT TRANSPORTATION SYSTEMS* (T-ITS), and involved in many international collaborations (projects, keynotes, and program boards) in EU, USA, China, India, and Australia.



Lóránt Tavasszy (Member, IEEE) received the Ph.D. degree in civil engineering from the Delft University of Technology (TU Delft) in 1996. From 1996 to 2016, he worked with the Dutch National Research Institute TNO as a Researcher, the Team Manager, and a Principal Scientist, and held part time chairs at the University of Nijmegen and TU Delft. He is currently a Full Professor in freight transport and logistics systems with TU Delft. His research involves freight transportation modeling at urban, national, and global level. Besides the textbook *Modelling Freight Transport*, he has published over 80 articles in various journals and over 150 papers in books and conference proceedings.

He also chairs the Scientific Committee of the World Conference for Transport Research Society (WCTRS) and is an Active Member of various international professional committees, including from the U.S. Transportation Research Board and the European Technology Platform for Logistics ALICE.



Maaïke Snelder received the degree in econometrics from Erasmus University in 2003 and the Ph.D. degree (*cum laude*) in robust road network design from the Delft University of Technology in 2010. She is currently a part-time Assistant Professor with the Department of Transport and Planning, Faculty of Civil Engineering and Geosciences, Delft University of Technology, and a Principal Scientist with TNO.